Journal of Photochemistry and Photobiology A: Chemistry 136 (2000) 103–109

Journal of Photochemistry and Photobiology A:Chemistry

www.elsevier.nl/locate/jphotochem

Photocatalytic oxidation of nitrogen monoxide over titanium(IV) oxide nanocrystals large size areas

Keiji Hashimoto [a,*], Kazuhiko Wasada [b], Naoji Toukai [a], Hiroshi Kominami [b], Yoshiya Kera [b]

[a] *Osaka Municipal Technical Research Institute, Morinomiya Joto-ku, Osaka 536-8553, Japan*

[b] *Department of Applied Chemistry, Faculty of Science and Engineering, Kinki University, Higashi-osaka, Osaka 577-0818, Japan*

Received 28 January 2000; received in revised form 12 April 2000; accepted 28 June 2000

Abstract

The titania prepared by high-temperature hydrolysis of titanium alkoxides in a hydrocarbon solvent is highly active for the photocatalytic oxidation of NO to NO_2 and NO_3. The photocatalytic oxidation activity decreases with an increase in post-calcination temperature of the titania. The surface area and crystal size of the titania make some contributions to the photocatalytic oxidation activity. IR spectra show that ultraviolet (UV) irradiation of the titania promotes the formation of nitrate species. The data of ESR and IR lead to the conclusions that NO, when irradiating the titania with UV rays, reacts with $O_2{}^-$ to form NO_2 and $NO_3{}^-$, but the radicals generated as a result of secondary products of O^- make no contribution to the photocatalytic oxidation. In addition, the concentration of free electron and $O_2{}^-$ decreases significantly with an increase in post-calcination temperature of the titania. © 2000 Elsevier Science S.A. All rights reserved.

Keywords: Photocatalytic oxidation; Nitrogen monoxide; Titanium alkoxide

1. Introduction

The worsening of one's living environment due to NO_x has constituted a serious social problem. It is very difficult to remove dilute NO_x gas which has been exhausted into an atmosphere from motor cars and manufactories. Sunlight is inexhaustible and free of charge, so that a photocatalytic technology using solar energy for the photocatalytic oxidation of NO may be capable of being a reasonable key to resolve the difficult problem. A plant and a micro-organism easily consume the products of the photocatalytic oxidation such as nitrite and nitrate ion as a raw material of nitrogen assimilation. This photocatalytic oxidation of NO using sunlight may hence achieve a practical removal of the dilute NO_x. An anatase-form titania is active for the photochemical reaction [1–4] and photodecomposition of poison compounds [5–11]. It is known that the crystal structure, surface area and/or surface hydroxyls of titania contribute to the activities for these photocatalytic reactions [12–15]. For some kinds of photocatalytic reactions, the recombination probability of electron and positive hole also might be one of the most significant factors controlling the activities [15]. However, a detailed contribution of the positive hole and electron to NO oxidation is obscure. On the other hand, we have already reported that titania prepared by high-temperature hydrolysis of titanium tetraalkoxides, $Ti(OR)_4$, in a hydrocarbon solvent is very active for the photocatalytic dehydrogenation of *sec*-propanol in an aqueous solution under deaerated conditions [16] and mineralization of acetic acid under aerated conditions [17]. We attempted to apply this titania to the photocatalytic oxidation of NO. In this paper, we report (1) the high activity of titania, (2) the formation of $O_2{}^-$ on irradiation of titania with ultraviolet (UV) rays, (3) the reactivity of $O_2{}^-$ with NO, and (4) the concentration of $O_2{}^-$ and free electron in titania.

2. Experimental

2.1. Materials

Titanium tetraethoxide and toluene were commercial materials of an analytical grade and were used without further purification. NO gas (100 ppm, He balance, Takachiho Kagaku Kogyo) was used.

2.1.1. Preparation of titanium oxide

Titanium oxide (Hycom TiO_2) was prepared according to the procedures previously described by H. Kominami et al. [18]; titanium(IV) butoxide (25 g) in toluene (70 ml) was hydrolyzed at 300°C for 2 h in an autoclave in the presence of water (10 ml) fed in a space separated from the alkoxide

---

[*] Corresponding author. Tel.: +81-6-6963-8040.

1010-6030/00/$ – see front matter © 2000 Elsevier Science S.A. All rights reserved.

PII: S1010-6030(00)00329-4

solution. The resulting slurry was filtrated, washed several times with acetone and dried in air at ambient temperature. As-prepared Hycom TiO_2 was then calcined at various temperatures under a flow of air (30 ml min^{-1}); the sample was heated at the rate of 10°C min^{-1} up to the desired temperature, kept at that temperature for 1 h and cooled to room temperature.

2.1.2. Photocatalytic oxidation

Photocatalytic oxidation was carried out in a fixed bed continuous flow reactor under atmospheric pressure: the reactor was made of a pyrex-glass equipped with an entrance window with a 100 mm inner diameter to irradiate the catalyst with UV rays; diffusion and uniform irradiation inside the reactor volume were accomplished by illuminating the plate of the window with an almost uniform radiation flux and making the interior side of the plate with a ground sample board. The catalyst, 0.12 g, was placed on a sample board in the reactor and treated at room temperature in an air stream to attain an equilibrium adsorption of NO. Air containing 10 ppm of NO at a flow rate of 110 ml min^{-1} was used as the reaction gas. The reaction product was analyzed on-line by NO_x meter. At first, the reaction gas was analyzed without UV irradiation of the titania after an adsorption equilibrium of NO was attained. The effect of UV irradiation on the photocatalytic oxidation was then studied: UV lamp (black light, 10 W h) was used. The pyrex-glass reactor makes no contribution to the photocatalytic oxidation.

2.1.3. Surface area

Surface area was determined by the BET method using nitrogen adsorption at −196°C.

2.1.4. X-ray powder diffraction (XRD) analysis

XRD patterns of the samples were recorded using a Rigaku Rint 2500 (Ni-filtered Cu Kα, 40 kV, 80 mA) equipped with a monochromater. The sample was mounted on a sample board and the measurements were carried out immediately.

2.1.5. FT-IR measurements

The FT-IR spectra were recorded by a Shimadzu FT-IR 8100 using a conventional IR cell connected to a vacuum line and adsorption apparatus. The sample (0.01 g) was pressed at 7.5 tonnes cm^{-2} using a pellet die to form a wafer with a 10 mm diameter and then placed in the in situ IR cell which allowed heating under vacuum. After the wafer was heated in vacuo for 1 h, the wafer was exposed to NO gas (1.5 kPa) at room temperature. FT-IR spectra of adsorbed NO were recorded at room temperature prior to oxygen exposure and UV irradiation. FT-IR spectra were then recorded after the oxygen exposure and UV irradiation.

2.1.6. ESR measurements

ESR spectra were recorded on a Japan Electron ESR analyzer using a conventional ESR tube connected to a vacuum line and adsorption apparatus. The ESR tube equipped with a vacuum cock was made of pyrex-glass with a 3 mm diameter. The titania (200 mg) was placed in the ESR tube and evacuated at a fixed temperature for 2 h. ESR spectra were recorded before UV irradiation of the titania and exposure to NO (0.1 kPa) and/or oxygen gas (0.1 kPa) or N_2O (0.1 kPa). After the exposure and UV irradiation, ESR spectra were then recorded at −150°C. Manganese marker was used as a standard. In a quantitative analysis of $O_2{}^{-}$, a silica loading of 0.5 wt.% of Cu^{2+} ions was used as a calibrator.

3. Results and discussion

The effect of post-calcination temperature on the photocatalytic oxidation was studied for the titania which was prepared by the hydrolysis of titanium tetraethoxide in a cyclohexane solvent, followed by calcination at different temperatures. The results are shown in Fig. 1. The titania calcined at 300°C is highly active for the photocatalytic oxidation, in comparison with an activity of representative commercial titania (P-25). The photocatalytic oxidation activity decreases with an increase in post-calcination temperature.

X-ray diffraction patterns for the titania calcined at various temperatures were recorded and are shown in Fig. 2. The titania calcined at 300°C contains a microcrystal, because the width of the XRD peaks is broad, compared to that at a temperature of more than 550°C. An anatase-form structure of titania is maintained up to 700°C and the rutile one increases above 700°C. The crystal size of anatase-form titania was determined on the basis of the half-width of the (1 0 1) diffraction peak using the Sherrer equation [19]. The results are summarized in Table 1. The elevation of the post-calcination temperature induces the increase in the crystal size of anatase-form titania.

The surface area of the titania was measured and is also summarized in Table 1. The increase in post-calcination temperature decreases the surface area of the titania. The activity

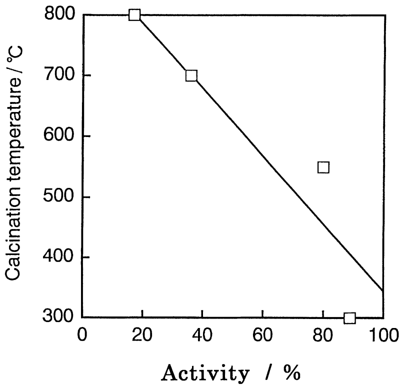

Fig. 1. Effect of calcination temperature on the photocatalytic oxidation activity. Catalyst: 0.12 g, NO: 10 ppm, air balance, flow rate: 110 ml min^{-1}, UV irradiation time: 2.0 h, reaction temperature: room temperature, black light: 10 W h.

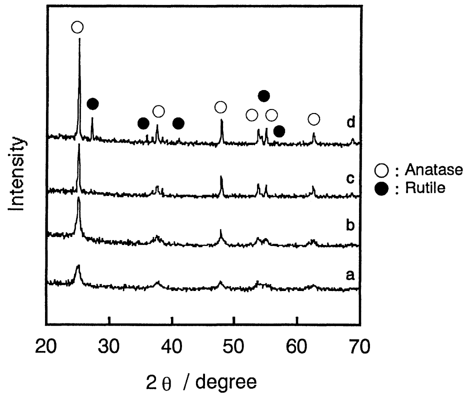

Fig. 2. X-ray diffraction patterns: (a) calcination at 300°C; (b) calcination at 550°C; (c) calcination at 700°C; (d) calcination at 800°C.

Table 1
Crystal size and surface area of the catalysts

Catalyst	Calcination temperature (°C)	Crystal type	Crystal size (nm)	Surface area ($m^2\,g^{-1}$)
TiO_2	300	Anatase	10	133
TiO_2	550	Anatase	18	78
TiO_2	700	Anatase	26	34
TiO_2	800	Anatase + rutile	47	8

of the photocatalytic oxidation over the anatase-form titania has a tendency to be higher in a higher surface area of the titania, although an amorphous-form titania (representative commercial amorphous-form titania, Idemitsu UF) having a high surface area has low activity for the photocatalytic oxidation. The effects of the surface area and crystal size on the photocatalytic oxidation activity are determined from the data in Table 1 and Fig. 1, and are shown in Fig. 3. The results indicate that the surface area and crystal size make some contributions to the photocatalytic oxidation.

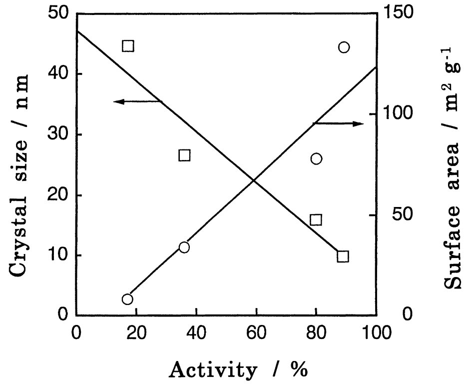

Fig. 3. Effect of the surface area and crystal size of the titania on the photocatalytic oxidation activity.

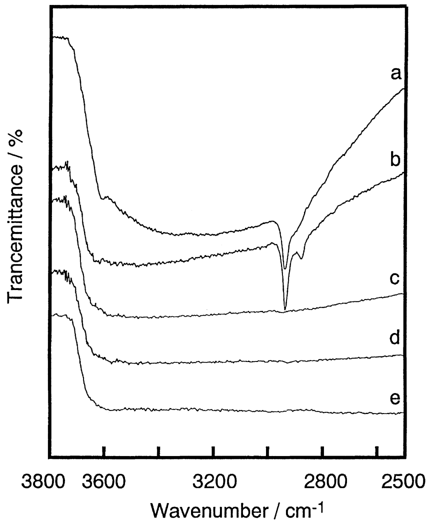

Fig. 4. FT-IR spectra in the range of 3800–2500 cm^{-1}: (a) without post-calcination; (b) calcination at 300°C; (c) calcination at 550°C; (d) calcination at 700°C; (e) calcination at 800°C.

FT-IR spectra in the range of 3800–2500 cm^{-1} were measured for the titania calcined at various temperatures and are shown in Fig. 4. The titania calcined at 300°C and without post-calcination gives two bands at 3600 and 3400 cm^{-1}, and has two bands in the range of 2800–3000 cm^{-1}. In the titania calcined above 550°C, the intensity of the band at about 3600 cm^{-1} decreases. Furthermore, the bands at about 3400 and 2800–3000 cm^{-1} are negligible. In the literature [20], a free hydroxyl group gives a sharp band at 3600–3700 cm^{-1}, and a hydroxyl group that has a hydrogen bonding gives a broad one around 3400 cm^{-1}. An organic compound exhibits a stretching vibration of the C–H bond at 2800–3100 cm^{-1} [20]. The titania calcined at a lower temperature has a higher intensity of the band due to hydroxyl groups than that at a higher temperature. This indicates that the amount of hydroxyl groups decreases with an increase in the post-calcination temperature. The titania prepared without post-calcination contains organic compounds which result from the decomposition of titanium alkoxide and/or hydrocarbon solvent.

FT-IR spectra of NO adsorbed on the titania were recorded and are shown in Fig. 5. In the absence of oxygen gas, the adsorption of NO on anatase-form titania gives the bands at 1605 (with a broad shoulder at 1640 cm^{-1}), 1583, 1487, 1477 (with a shoulder at 1460 cm^{-1}), 1296, and 1266 cm^{-1} (with a shoulder at 1252 cm^{-1}), whereas in the presence of oxygen gas, that gives the bands at 1608 (with a broad shoulder 1640 cm^{-1}), 1586, 1487 (with a shoulder at 1477 cm^{-1}), 1296 and 1267 cm^{-1} (with a shoulder at 1252 cm^{-1}). The adsorption of NO in the presence of oxygen gas, followed by 20 min of UV irradiation, leads to the appearance of the bands at 1380, 1360, and 1252 cm^{-1}. In the literature [21–24], the bands at 1650–1550 and 1250–1180 cm^{-1} can be assigned to the ν_3 vibration of bridge and bidentate nitrates ($\Delta\nu_3 = 480–200\,cm^{-1}$) on anatase-form titania and titanium ion, whereas those at 1550–1500 and 1290–1250 cm^{-1} correspond to monoden-

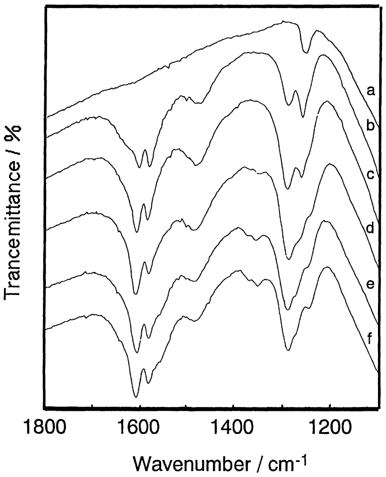

Fig. 5. FT-IR spectra of NO_x species on the titania: (a) evacuation at 400°C for 2 h; (b) exposure to 0.1 kPa of NO; (c) exposure to NO in the presence of oxygen; (d) UV irradiation for 10 min in the presence of oxygen and NO; (e) UV irradiation for 30 min in the presence of oxygen and NO; (f) UV irradiation for 60 min in the presence of oxygen and NO.

tate nitrates ($\Delta\nu_3 = 280$–$190\,\mathrm{cm}^{-1}$). IR absorption, arising from the ν_3 vibration of nitrate ions, occurs in the general region around 1450–1250 cm^{-1}. The adsorption of NO on anatase-form titania gives no bands in the 1900–1700 cm^{-1} regions, which would be characteristic of nitrosyl species [25,26]. Moreover, IR adsorption, arising from a bending vibration of H_2O, occurs in the general region around 1640 cm^{-1}. The bands at 1608–1605, 1586–1583, and 1297 cm^{-1} are attributable to the ν_3 vibration of bidentate nitrite. The results in the absence of oxygen gas indicate that NO adsorption causes nitrosyl species to be attached to the surface oxygen of titania, resulting in bidentate nitrate. A similar formation of nitrate has been observed for NO_2 adsorption on anatase-form titania [21]. This formation has been explained by NO_2 adsorption, taking into account the disproportion of NO_2 which proceeded on the anatase Lewis acid sites [21]:

$$\mathrm{Ti^{4+}\text{–}O^{2-} + 2NO_2 \rightarrow Ti^{4+}(NO_3{}^{-})\text{–}O^{2-}(NO^{+})} \qquad (1)$$

The bands at 1483, 1477, and 1267 cm^{-1} are attributable to the ν_3 vibration of monodentate nitrite. The results in the presence of oxygen gas indicate that NO adsorption causes nitrite to be formed with adsorbed oxygen, resulting in monodentate nitrate. The NO adsorption simultaneously accompanies the formation of water with monodentate nitrate as shown in Fig. 5. A similar formation of water has also been observed for NO_2 adsorption on anatase-form titania [21,27]. The explanation takes account into the interaction of adsorbed NO_2 with the Ti–OH group having a basic character to induce the following disproportion [21,27]:

$$\mathrm{3NO_2 + 2OH^{-} \rightarrow 2NO_3{}^{-} + NO + H_2O} \qquad (2)$$

The bands at 1380, 1360, and 1252 cm^{-1} are attributed to the ν_3 vibration of nitrate ions. UV irradiation of the titania significantly promotes a formation of nitrate with adsorbed oxygen via the above reaction scheme (1) and/or (2).

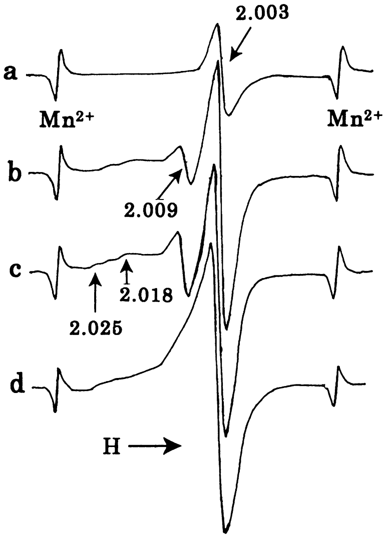

Fig. 6. ESR spectra of oxygen radicals on the titania: (a) evacuation at 400°C for 2 h; (b) exposure at room temperature to 0.1 kPa of oxygen; (c) UV irradiation at room temperature for 20 min in the presence of oxygen; (d) exposure at 200°C for 15 s to 0.1 kPa of N_2O.

On irradiation of the titania with UV rays, ESR spectra of the catalysts were recorded at −150°C in the presence of oxygen and/or NO. These results are shown in Figs. 6 and 7. ESR measurements for the catalyst give at least two kinds of spectrum patterns: one, giving an isotropic spectrum, A, has a g-tensor of $g = 2.003$, and second, giving an anisotropic spectrum, B, has a g-tensor of $g_1 = 2.018$–2.025, $g_2 = 2.009$ and $g_3 = 2.003$. In the literature [28–33], a spectrum of $O_2{}^{-}$ adsorbed on TiO_2 appears at $g_1 = 2.018$–2.025, $g_2 = 2.009$ and $g_3 = 2.001$–2.003. The value of g_1 for $O_2{}^{-}$ is changed by the environment of titanium atom attached to $O_2{}^{-}$ [33]. Signal B at $g_1 = 2.018$–2.025, $g_2 = 2.009$ and $g_3 = 2.003$ is attributed to $O_2{}^{-}$ adsorbed on the different sites of the titania. Titanium(III) gives an anisotropic signal

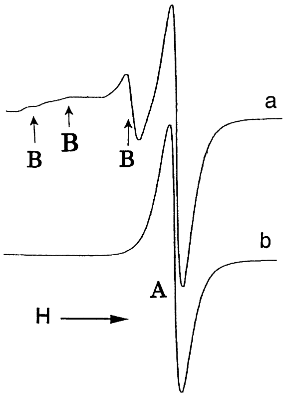

Fig. 7. Reactivity of $O_2{}^{-}$ with NO: (a) evacuation at room temperature for 20 min after UV irradiation in the presence of oxygen; (b) exposure at room temperature to 0.1 kPa of NO.

at $(g_1, g_2, g_3) \leqq 1.992$ [30,31,34,35]. Therefore, the g-value of A refuses the probability that signal A is assigned to titanium(III). UV irradiation significantly causes the intensities of signals A and B to be increased in the presence of oxygen. In addition, adsorption of N_2O leads to the appearance of the signal at $g = 2.003$. In particular, a 15 s exposure of N_2O at 200°C under 0.1 kPa of N_2O to the titania significantly increases the intensity of the signal at $g = 2.003$ (Fig. 6d). Signal A increases on irradiation of the titania with UV rays in the presence of oxygen, whereas its intensity scarcely changes in the absence of oxygen. The same signal is observed by adsorption of N_2O. The decomposition of N_2O over metal oxides and/or metal generally generates the O^- radical and dinitrogen [36–38]. The isotropic spectrum at $g = 2.003$ was attributed to O^- by T. Kwan, [36] and J.H. van Hooff, [39], but the radical of O^- in orthorhombic or tetragonal symmetry theoretically has an anisotropic g-tensor [40]. The spectrum is due to a radical generated as a result of secondary products via O^-.

Signal B disappears on exposure at room temperature to NO gas, whereas the intensity of signal A scarcely changes (Fig. 7). The results indicate that O_2^- oxidizes NO at room temperature, but the free radical scarcely reacts with NO. The results indicate that UV irradiation in the presence of oxygen gives O_2^- and the free radical in the titania. The species of O_2^- react with NO at room temperature to form NO_2 and NO_3^-. When no UV rays are radiated, a little amount of the radical and O_2^- are observed in the titania calcined at temperature less than 550°C. This is explainable in terms of lattice defects that are generally generated on preparation of titania: the presence of defects on the titania surface have been demonstrated by computer chemistry [41].

The amount of O_2^- induced by 20 min of irradiation of the titania with UV rays was determined for the titania calcined at different temperatures. The results are shown in Fig. 8. The photocatalytic oxidation activity corresponds well to the amount of O_2^- generated by UV irradiation. The amount of O_2^- decreases with an increase in post-calcination temperature.

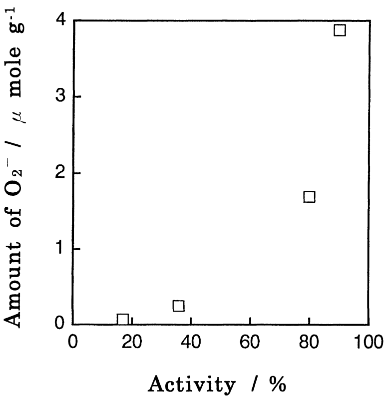

Fig. 8. Effect of the amount of O_2^- on the photocatalytic oxidation activity.

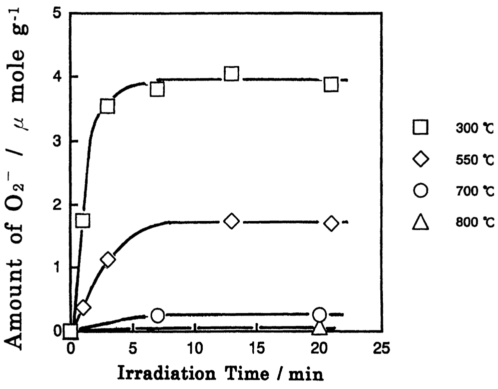

Fig. 9. Effect of UV irradiation time on the amount of O_2^-. □: calcination at 300°C, ◇: calcination at 550°C, ○: calcination at 700°C, △: calcination at 800°C.

The variation of the amount of O_2^- with UV radiation time-on-stream was studied and is shown in Fig. 9. The amount of O_2^- increases with an increase in the UV irradiation time up to 15 min, and attains an asymptotic value for any further time-period. The initial rates of O_2^- formation for the catalyst calcined at 300, 550, 700, and 800°C are determined to be 2.9, 0.80, 0.06, and 0.01 μmole min^{-1} g-cat^{-1}, respectively (Table 2); the values of the initial rates are derived as the UV irradiation time approaches 0. The rate of formation and the rate of recombination between a positive hole and a free electron are considered to be very rapid, and so the equilibrium between the formation and recombination is instantaneously attained on irradiation of the titania with UV rays:

$$\mathrm{Ti} \overset{h\nu}{\leftrightarrows} \text{positive hole} + e$$

The asymptotic values in Fig. 9 indicate that equilibrium between the formation and reverse reaction of O_2^- is attained. For convenience, we assume a first-order rate equation of O_2^- formation and reverse reaction for each concentration. The rates of formation and reverse reaction are expressed in the following equations:

Table 2
Rate parameter[a]

Catalyst	Calcination temperature (°C)	$R_{f\alpha}$ (μmole min^{-1})	$[O_2^-]_\alpha$ (μmole g^{-1})	$R(e)_i$	$R(k_2)_i$
TiO_2	300	2.9	7.2	1.00	1.00
TiO_2	550	0.80	3.7	0.48	0.54
TiO_2	700	0.06	0.25	0.05	0.59
TiO_2	800	0.01	0.07	0.06	0.35

[a] $R_{f\alpha}$ — rate of formation of O_2^- for the titania calcined at α°C; $[O_2^-]_\alpha$ — concentration of O_2^- for the titania calcined at α°C; $R(e)_i$ — relative ratio of $[e]_\alpha$ to $[e]_{300}$, where $[e]_\alpha$ and $[e]_{300}$ stand for the number of free electrons for the titania calcined at α and 300°C, respectively; $R(k_2)_i$ — relative ratio of $(k_2)_\alpha$ to $(k_2)_{300}$, where $(k_2)_\alpha$ and $(k_2)_{300}$ are the rate constants of the reverse reaction for the titania calcined at α and 300°C, respectively.

$$R_{\mathrm{f}i} = k_{1i}[\mathrm{e}]_i[\mathrm{O_2}] \tag{3}$$

$$R_{\mathrm{r}i} = k_{2i}[\mathrm{O_2}^-]_i \tag{4}$$

where $R_{\mathrm{f}i}$, $R_{\mathrm{r}i}$, k_{1i}, k_{2i}, $[\mathrm{O_2}]_i$, $[\mathrm{O_2}^-]_i$ and $[\mathrm{e}]_i$ are the rate of formation of $\mathrm{O_2}^-$, its reverse reaction rate, the rate constant of formation, the rate constant of the reverse reaction, the concentration of adsorbed $\mathrm{O_2}$, the concentration of $\mathrm{O_2}^-$ and the number of free electrons, respectively. Assuming a uniform surface in the titania, $[\mathrm{O_2}]_i$ is represented by a Langmuir-type equation:

$$[\mathrm{O_2}]_i = \frac{S_\mathrm{t} K[P_{\mathrm{O_2}}]}{1 + K[P_{\mathrm{O_2}}]} \tag{5}$$

where K, $[P_{\mathrm{O_2}}]_i$ and S_t are the equilibrium constant of $\mathrm{O_2}$ adsorption, the partial pressure of $\mathrm{O_2}$ and the surface area of the titania, respectively. Eq. (3) is rearranged using a Langmiur-type equation:

$$R_{\mathrm{f}i} = \frac{k_{1i} S_\mathrm{t}[\mathrm{e}]_i K[P_{\mathrm{O_2}}]}{1 + K[P_{\mathrm{O_2}}]} \tag{6}$$

The ratio of the rates of formation for the two kinds of titania calcined at different temperatures represents the existence ratio of $[\mathrm{e}]_i$. If two kinds of the titania calcined at different temperature are expressed by the sign of α and β, their rates of formation are expressed by the sign of $R_{\mathrm{f}\alpha}$ and $R_{\mathrm{f}\beta}$. $R_{\mathrm{f}\alpha}$ and $R_{\mathrm{f}\beta}$ are determined from the initial rates of formation (Fig. 9). In a steady state, $R_{\mathrm{f}i}$ is equal to $R_{\mathrm{r}i}$. Assuming K to be constant for the titania, the ratio of the rate of formation, $R_{\mathrm{f}\alpha}/R_{\mathrm{f}\beta}$, and the ratio of reverse reaction, $R_{\mathrm{r}\alpha}/R_{\mathrm{r}\beta}$, for each titania, are expressed in the following equations:

$$\frac{R_{\mathrm{f}\alpha}}{R_{\mathrm{f}\beta}} = \frac{k_{1\alpha} S_{\mathrm{t}\alpha}[\mathrm{e}]_\alpha K[P_{\mathrm{O_2}}]/(1 + K[P_{\mathrm{O_2}}])}{k_{1\beta} S_{\mathrm{t}\beta}[\mathrm{e}]_\beta K[P_{\mathrm{O_2}}]/(1 + K[P_{\mathrm{O_2}}])} = \frac{S_{\mathrm{t}\alpha}[\mathrm{e}]_\alpha}{S_{\mathrm{t}\beta}[\mathrm{e}]_\beta} \tag{7}$$

$$\frac{R_{\mathrm{r}\alpha}}{R_{\mathrm{r}\beta}} = \frac{k_{2\alpha}[\mathrm{O_2}^-]_\alpha}{k_{2\beta}[\mathrm{O_2}^-]_\beta} \tag{8}$$

If we substitute the values of $R_{\mathrm{f}\alpha}$, $R_{\mathrm{f}\beta}$, $S_{\mathrm{t}\alpha}$, and $S_{\mathrm{t}\beta}$ into Eq. (7), the ratio of $[\mathrm{e}]_\alpha$ to $[\mathrm{e}]_\beta$ is calculated, and is summarized in Table 2. The concentration of free electrons decreases with an increase in the post-calcination temperature. Substituting the value of $[\mathrm{O_2}^-]_\alpha$ and $[\mathrm{O_2}^-]_\beta$ into Eq. (8), $k_{2\alpha}/k_{2\beta}$ is determined and is also summarized in Table 2. The increase in the post-calcination temperature significantly decreases $[\mathrm{O_2}^-]$ and $[\mathrm{e}]$ in the titania. The result suggests a higher rate of formation of positive hole and free electron and/or a lower rate of recombination at a lower temperature of post-calcination. Our coworker reported that effects of the post-calcination temperature on several photocatalytic reactions could be interpreted reasonably by taking the number of electrons (or holes) needed to complete the photocatalytic reaction into account and that a low recombination probability seemed to be desirable for the photocatalytic reaction of multi-electron processes [42]. The results lead to the conclusion that a low recombination probability of the titania leads to a high content of $\mathrm{O_2}^-$ to be formed: the lower the recombination probability of the titania, the more is the amount of trapped electrons, followed by the formation of $\mathrm{O_2}^-$.

4. Conclusion

Photocatalytic oxidation of NO to $\mathrm{NO_2}$ and $\mathrm{NO_3}^-$ with oxygen was studied for titania which was prepared by the hydrolysis of titanium alkoxide in a hydrocarbon solvent, followed by calcination at various temperatures. The titania calcined at 300°C is highly active for the photocatalytic oxidation, in comparison with representative commercial titania, P-25 (Zegussa). The photocatalytic oxidation activity decreases with an increase in post-calcination temperature. The data of XRD and BET surface area indicate that the crystal size and surface area of anatase-form titania decrease with an increase in the post-calcination temperature. The results support the idea that the surface area and crystal size of the titania make some contributions to the photocatalytic oxidation. UV irradiation of the titania in the presence of oxygen and NO leads the appearance of the bands at 1380, 1360 and 1252 cm^{-1} assigned to the ν_3 vibration of nitrates. IR spectra show that UV irradiation promotes the oxidation of NO with oxygen and forms nitrate species. The data of ESR measurements for oxygen radicals show that UV irradiation increases the amount of $\mathrm{O_2}^-$ adsorbed on the surface of the titania in the presence of oxygen. The species of $\mathrm{O_2}^-$ vanish simultaneously on exposure to NO, whereas the spectrum intensity of the radical generated as a result of secondary products of O^- does not change. The amount of $\mathrm{O_2}^-$ generated by UV irradiation is proportional to the photocatalytic oxidation activity of the titania. The results lead to the conclusion that $\mathrm{O_2}^-$ react easily with NO, that is, the radicals of $\mathrm{O_2}^-$ generated by UV irradiation contribute to the acceleration of the photocatalytic oxidation. The rate of formation of $\mathrm{O_2}^-$ and the amount of free electrons induced by UV irradiation decrease significantly with an increase in the post-calcination temperature. The results lead to the conclusion that a low rate of electron–hole recombination for Hycom $\mathrm{TiO_2}$ enhances the photocatalytic oxidation of NO.

References

[1] A. Fujishima, K. Honda, Nature 238 (1972) 37.
[2] S. Kodama, S. Yagi, J. Chem. Soc., Faraday Trans. 88 (1992) 1685.
[3] M.L. Sauer, D.F. Ollis, J. Catal. 149 (1994) 81.
[4] K. Sayama, H. Arakawa, J. Chem. Soc., Faraday Trans. 93 (1997) 1647.
[5] A.L. Pruden, D.F. Ollis, J. Catal. 82 (1983) 404.
[6] R.W. Matthews, J. Chem. Soc., Faraday Trans. 80 (1984) 457.
[7] H. Gerischer, in: D.F. Ollis, H. Al-Ekabi (Eds.), Photocatalytic Purification and Treatment of Water and Air, Elsevier, Amsterdam, New York, 1993, p. 1.
[8] C. Minero, E. Pelizzetti, S. Malato, J. Blanco, J. Solar Energy 56 (1996) 421.
[9] M.I. Cabrera, A.C. Negro, O.M. Alfano, A.E. Cassano, J. Catal. 172 (1997) 380.

[10] N.W. Cant, J.R. Cole, J. Catal. 134 (1992) 317.
[11] M.R. Hoffmann, S.T. Martin, W. Choi, D.W. Bahnemann, Chem. Rev. 95 (1995) 69.
[12] S. Sato, Hyoumen 28 (1990) 427.
[13] B. Ohtani, S.-i. Nishimoto, J. Phys. Chem. 97 (1993) 920.
[14] B. Ohtani, Y. Ogawa, S.-i. Nishimoto, J. Phys. Chem. B 101 (1997) 3746.
[15] B. Ohtani, R.M. Bowman, D.P. Colombo Jr., H. Kominami, H. Noguchi, K. Uosaki, Chem. Lett. (1998) 579.
[16] H. Kominami, T. Matsuura, K. Iwai, B. Ohtani, S. Nishimoto, Y. Kera, Chem. Lett. (1995) 693.
[17] H. Kominami, J. Kato, M. Kohno, Y. Kera, B. Ohtani, Chem. Lett. (1996) 1051.
[18] H. Kominami, Y. Takada, H. Yamagiwa, Y. Kera, M. Inoue, T. Inui, J. Mater. Sci. Lett. 15 (1996) 197.
[19] P. Scherrer, Göttinger Nachrichten 2 (1918) 98.
[20] R.M. Silverstein, G.C. Bassler, Spectrometric Identification of Organic Compounds, Wiley, New York, 1963, pp. 49–70.
[21] M.M. Kantcheva, V.Ph. Bushev, K.I. Hadjivanov, J. Chem. Soc., Faraday Trans. 88 (20) (1992) 3087.
[22] T.J. Dines, C.H. Rochester, A.M. Ward, J. Chem. Soc., Faraday Trans. 87 (4) (1991) 643.
[23] M.M. Kantcheva, V. Bushev, D. Klissurski, J. Catal. 145 (1994) 96.
[24] S.D. Ross, Inorganic Infrared and Raman Spectra, McGraw-Hill, Maidenhead, UK, 1972, p. 152.
[25] M.L. Hair, J. Phys. Chem. 74 (1970) 1290.
[26] K. Nakamoto, Infrared and Raman Spectra of Inorganic and Coordination Compounds, Wiley, New York, 1988, p. 206.
[27] K. Hadjiivanov, D. Klissurski, A. Davidov, J. Catal. 116 (1989) 498.
[28] C. Naccache, P. Meriaudeau, M. Che, A.J. Tench, Trans. Faraday Soc. 67 (1971) 506.
[29] P. Meriaudeau, J.C. Vedrine, J. Chem. Soc., Faraday Trans. 2 72 (1976) 472.
[30] R.F. Howe, M. Grätzel, J. Phys. Chem. 89 (1985) 4495.
[31] R.F. Howe, M. Grätzel, J. Phys. Chem. 91 (1987) 3906.
[32] Y. Nakaoka, Y. Nosaka, J. Photochem. Photobiol. A: Chem. 110 (1997) 299.
[33] H. Kanai, M. Shono, S. Imamura, H. Kobayashi, J. Mol. Catal. A: Chem. 130 (1998) 187.
[34] R.C. Wilson, R.J. Myer, J. Chem. Phys. 64 (1974) 2208.
[35] A. Avudaithai, T.R.N. Kutty, Mater. Res. Bull. 23 (1988) 1675.
[36] H. Horiguchi, M. Setaka, T. Kwan, in: Proceedings of the Fourth International Congress on Catalysis, Moscow Preprint No. 5, 1968.
[37] N.B. Wong, J.H. Lunsford, J. Chem. Phys. 55 (1971) 3007.
[38] V.M. Vorotyntsev, V.A. Shvets, V.B. Kazanskii, Kinet. Katal. 12 (1971) 678.
[39] J.H.C. van Hooff, J. Catal. 11 (1968) 277.
[40] J.H. Lunford, Advances of Catalysis, Vol. 22, Academic Press, New York and London, 1972, p. 332.
[41] M. Ramamoorthy, R.D. King-Smith, D. Vanderbilt, Phys. Rev. B: Condens. Matter 49 (1994) 7709.
[42] H. Kominami, S. Murakami, Y. Kera, B. Ohtani, Catal. Lett. 56 (1998) 125.